3.3.2.1 Research Paper Published in UGC Care Listed Journals

Colloids and Surfaces A 582 (2019) 123883

Contents lists available at ScienceDirect

Colloids and Surfaces A

journal homepage: www.elsevier.com/locate/colsurfa

Sustained release insect repellent microcapsules using modified cellulose nanofibers (mCNF) as pickering emulsifier

Sandip L. Kadam[a,b], Prashant Yadav[a,b], Siddhant Bhutkar[a], Vishal D. Patil[a], Parshuram G. Shukla[a], Kadhiravan Shanmuganathan[a,b,*]

[a] Polymer Science and Engineering Division, CSIR - National Chemical Laboratory, Dr. Homi Bhabha Road, Pune 411008, India
[b] Academy of Scientific and Innovative Research, CSIR - National Chemical Laboratory Campus, Dr. Homi Bhabha Road, Pune 411008, India

GRAPHICAL ABSTRACT

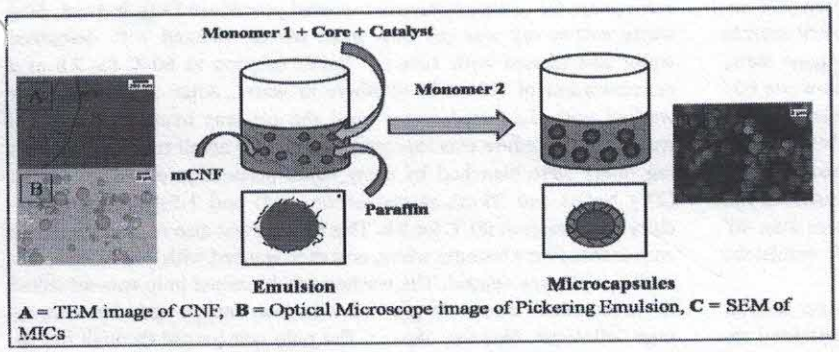

A = TEM image of CNF, **B** = Optical Microscope image of Pickering Emulsion, **C** = SEM of MICs

ARTICLE INFO

Keywords:
Pickering emulsion
Cellulose nanofiber
Nanoparticle
Microcapsules
Controlled release
Nanocomposite

ABSTRACT

We report here an approach to encapsulate *N, N*-diethyl-3-methylbenzamide (DEET), an insect repellent, through interfacial polycondensation using modified cellulose nanofiber (CNF) as pickering emulsifier. We found that stearic acid functionalized CNF (mCNF) can be used to form stable pickering emulsions (oil-in-oil and water-in-oil), and further encapsulate DEET using interfacial polycondensation with very high encapsulation efficiency of about 98%. Another major advantage of this approach is that mCNF can act both as pickering emulsifier and also strengthen the barrier properties of microcapsules resulting in significant reduction in release rate of DEET. Interpretation of the release profiles using standard mathematical models proposed by Ritger-Peppas show a factor of three reduction in release rate constant for the microcapsules reinforced with mCNF.

1. Introduction

Sustained release of active ingredients by microencapsulation techniques has elicited tremendous interest in diverse applications such as pharmaceuticals, agrochemicals, paints, coatings, consumer products, textiles etc. [1,2]. Microencapsulation enables safer and efficient handling of chemicals. It can also help to reduce the degradation and leaching of toxic chemicals [3]. Encapsulation can be achieved by different physical methods such as spray drying, solvent evaporation, layer-by-layer (L-B-L) assembly and chemical methods such as sol-gel encapsulation, in-situ/interfacial polymerization etc. [4]. Various polymeric wall forming materials such as urea-formaldehyde (U-F),

* Corresponding author at: Polymer and Advanced Materials Laboratory, Polymer Science and Engineering Division, CSIR-National Chemical Laboratory, Pune, India
E-mail address: k.shanmuganathan@ncl.res.in (K. Shanmuganathan).

https://doi.org/10.1016/j.colsurfa.2019.123883
Received 24 June 2019; Received in revised form 28 August 2019; Accepted 28 August 2019
Available online 29 August 2019
0927-7757/

melamine-formaldehyde (M-F), polystyrene (PS), polyurethane, polyurea etc. have been employed to encapsulate active ingredients [5]. Among all other chemical methods, interfacial polymerization is attractive for microencapsulation due to the ability to achieve high loading efficiency of active ingredient [6–8].

Encapsulation of active ingredient using interfacial polymerization involves formation of a stable emulsion, following which the reaction of monomers at the interface of dispersed phase and continuous phase leads to the formation of a polymeric wall around the active ingredient. Polymeric surfactants are typically used to stabilize emulsions. In recent years, there has been significant research interest in using solid nanoparticles to stabilize emulsions (pickering emulsions) [9–11]. This helps to minimize adverse effects such as irritancy and hemolytic behavior, while also rendering more resistance to coalescence as compared to emulsions stabilized by surfactants. Some of the solid particles which have been used as pickering emulsifiers include silica [12,13], clay [14], barium sulfate [15], carbon black [16] and nanocellulose [17–20]. Among these, nanocellulose has gained attention as a bio-based, abundant, biodegradable, non-toxic, easily functionalizable nanomaterial that can be isolated from food waste and other plant sources such as sugarcane bagasse, cotton linters, wheat straw, banana stem, etc. Hydrophilic nanocellulose can be used to stabilize oil-in-water (O/W) emulsions while hydrophobic nanocellulose leads to stable water-in-oil (W/O) emulsions [21,22]. Wettability of the solid emulsifier at the interface is a very important variable and can be characterized by water contact angle (θ). If θ is less than 90°, particles prefer to reside in the water phase and stabilize O/W emulsions, and when θ is more than 90° particles prefer to reside in oil phase and stabilize W/O emulsions [8,23,24].

The term "controlled release" encompasses various aspects such as immediate release [25], target specific delivery [26] or sustained release [27,28]. Our work was aimed at preparing sustained release insect repellant formulations. Herein, we have made an attempt to prepare surfactant free W/O and O/O emulsions stabilized solely by stearic acid modified cellulose nanofibers (mCNF). We have used this as a platform to prepare polyurethane microcapsules using interfacial polycondensation and thereby encapsulate oil insoluble and water sensitive actives such as DEET, which is considered as a safer and effective insect repellant. The percutaneous absorption of DEET reduces its efficiency as an insect repellant. Microencapsulation could be a promising approach to inhibit DEET absorption into skin while ensuring prolonged effect of DEET in insect repellant formulations. Although few reports are available on microencapsulation of DEET [29,30], they are not based on pickering emulsions or nanocomposite microcapsules by interfacial polycondensation, a process that can lead to high encapsulation efficiency. Here, we report on the encapsulation of DEET by interfacial polycondensation using mCNF as pickering emulsifier. The advantage of this system is that in addition to acting as pickering emulsifier, mCNF also strengthens the barrier properties resulting in significant reduction in the release rate of active ingredients. Few recent reports have demonstrated the use of nanocellulose as pickering emulsifier. Stenius et al. [11] reported the preparation of W/O emulsions stabilized by hydrophobized microfibrillated cellulose and studied emulsion stability. Sebe et al [31]. reported the use of cinnamate modified nanocellulose as an inverse pickering emulsifier at water/toluene interface to obtain silica colloidosomes. However, the use of modified nanocellulose fibers to stabilize both O/O and W/O emulsions and the preparation of sustained release DEET microcapsules by interfacial polycondensation has not been reported before. We report here a systematic investigation of these particle stabilized microcapsules and their sustained release properties (Scheme 1).

2. Materials and methods

Sodium hydroxide (NaOH), sodium hypochlorite (4 wt%), glacial acetic acid (CH_3COOH), tosyl chloride (TsCl), stearic acid, and methanol (AR grade) were procured from Leonid chemicals Pvt. Ltd. Pyridine (Emparta grade), ethylene glycol (EG), DEET, dibutyl tin dilaurate (DBTDL) and liquid paraffin (heavy) oil, and petroleum ether (distillation range 65–70 °C) were procured from Merck chemicals. Absolute ethanol (99.99%) was procured from Changshu Hongsheng Fine Chemicals Co. Ltd. For the preparation of nanocellulose fibers, waste cotton rag was collected from local market. Toluene-2, 4-diisocyanate (technical grade (80%) (TDI), and fumed silica powder (0.007 μm) were purchased from Sigma Aldrich, USA. Hypermer A60 surfactant was obtained from Uniquema, UK. All chemicals were used as received.

2.1. Isolation of cellulose nanofibers (NF) from waste cotton rag

Preparation of cellulose nanofibers involves two steps. First, a chemical pretreatment is performed to remove hemicellulose, lignin etc. followed by size reduction of cellulose fibers by mechanical or chemical methods [32,33]. The cellulose nanofibers used in this work were prepared using previously reported procedure [34]. In brief, 50 g waste cotton rag was cut into small pieces, cleaned with deionized water and treated with 10% aq. NaOH solution at 60 °C for 2 h at a concentration of 3.3 wt % of fibers in water. After 2 h, fibers were washed with deionized water until the pH was neutral. This alkali treatment procedure was repeated twice. After alkali treatment, cotton rag fibers were bleached by using equal proportion of acetate buffer (27 g NaOH and 75 mL glacial acetic acid) and 1.5% sodium hypochlorite in water at 80 °C for 2 h. This process was also repeated twice to ensure that fibers become white, and then washed with deionized water until the pH was neutral. The washed and bleached pulp was subjected to mechanical shear in an ultra-friction micro grinder (Super-massColloider®, Masuko, Japan). The pulp was passed through the rotating grinding stones at 1500 rpm in multiple cycles with decreasing gap between the two grinding stones to obtain fibers of diameter less than 100 nm [35]. The obtained nanofibrils were lyophilized using Labconco lyophilizer and stored for further use. The size of the fibers was confirmed by Transmission Electron Microscopy (TEM).

2.2. Preparation of modified cellulose nanofibers (mCNF)

mCNF used in this work was prepared using procedure reported earlier [36]. In brief, 13 g of dry CNF (0.080 mol glucopyranose units) obtained by lyophilization was taken in a 3-necked round bottomed flask with 500 mL pyridine. After complete dispersion of CNFs in pyridine, 91 g TsCl (0.48 mol) was added with nitrogen purging and continuous agitation. After complete dissolution of TsCl, 136 g of stearic acid (0.48 mol) was added slowly into the mixture over a time span of 30 min. Then the temperature of the reaction mixture was raised to 50 °C and stirred continuously for 3 h. After this process, the reaction mixture was allowed to cool to room temperature. The fibers were then centrifuged and washed with ethanol at least 5 times. The fibers were dried at room temperature in fume hood. After drying, the fibers were Soxhlet-extracted with methanol initially for 2 h, and then the solvent was replaced with fresh methanol and again extracted for another 12 h to eliminate any impurities on the surface of mCNF. Finally, the mCNFs were removed, washed with ethanol and dried for 15 h in vacuum. Obtained modified fibers were characterized using FTIR, and ^{13}C-CP/MAS solid state NMR. mCNFs obtained by this process was stored as dry fibers and used for further experiments.

2.3. Preparation of polyurethane microcapsules using DEET as active ingredient and mCNF as Pickering emulsifier

Polyurethane microcapsules (MICs) were prepared using interfacial polycondensation in non-aqueous medium [37]. Oil-in-oil emulsion of DEET was prepared using mCNF as pickering emulsifier. mCNF was first homogenized in paraffin oil using MICCRA D-9 homogenizer at

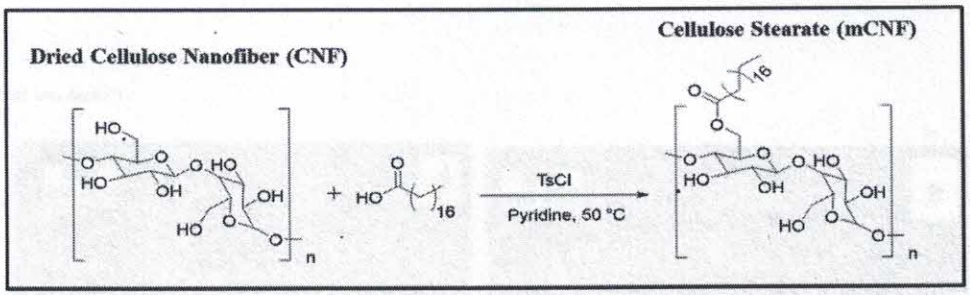

Scheme 1. Preparation of modified cellulose nanofibers (mCNF) with stearic acid.

11,000 rpm for 5 min to obtain homogeneous dispersion of mCNF. The content of mCNF was varied from 0.5 to 2 wt % with respect to paraffin oil. Further, the dispersed phase containing a mixture of 2.105 g (0.01207 mmol) of TDI, 0.2 g of DBTDL (1% solution in paraffin oil) and 2.6 g of DEET was added to the continuous medium. This mixture was further homogenized for 5 min at 11,000 rpm to obtain a stable emulsion.

This emulsion was stirred with an over-head stirrer at 1000 rpm at room temperature. After 20 min, 0.5 g (0.00805 mmol) of ethylene glycol was added drop wise. After the addition, temperature of the system was raised to 60 °C and maintained for 5 h. The reaction medium was then cooled to 28 °C and stirring speed was reduced to 600 rpm. These conditions were maintained for next 15 h. Then the milky suspension was centrifuged, filtered and subjected to multiple washing with petroluem ether. Pristine microcapsules were also prepared using above mentioned protocol but using conventional surfactant i.e. Hypermer A60 (1 wt%) instead of the pickering emulsifier mCNF.

3. Characterization

3.1. Morphology and chemical characterization

TEM was used to determine the dimensions of CNF. Sample was prepared by stirrring CNF in water (0.05 mg/mL) for 6 h and then sonicating for 1 h in a water bath. mCNF was dispersed in dichloromethane instead of water as per above conditions. The uniformly dispersed sample was drop casted on a carbon coated copper grid with 200 mesh size and dried overnight in a fume hood at ambient conditions. The data was acquired using FEI-Tecnai-F20 electron microscope operating at 200 kV. The reaction of CNF with stearic acid was monitored using FTIR and ^{13}C-CPMAS solid-state NMR. FTIR was used in transmission mode to confirm the reaction between stearic acid and CNF. KBr pellets were prepared using the standard procedure, and FTIR spectrum was acquired using Perkin Elmer Q5000 GX IR instrument with 32 scans and resolution of 4 cm^{-1}. For solid-state^{13}C Cross polarization/Magic Angle Spinning (CP/MAS) NMR, completely dried sample powder was analyzed using Bruker Spectrometer (400 MHz) broadband 4 mm CP/MAS probe. The contact angle of CNF and mCNF surfaces was measured using Kruss drop shape analyzer. For this analysis, CNF and mCNF were molded into films in a hydraulic polymer press (Model PF-M 15) at 70 °C and 2000 psi. The morphology of the microcapsules was analyzed using optical microscopy and scanning electron microscopy. Olympus BX-60, USA optical microscope fitted with Olympus SC30 digital camera was used to monitor capsule formation. Scanning Electron Microscope (SEM) (E-SEM, Quanta 300) was used to probe the morphology of MICs. Samples were sputter coated with gold before SEM imaging to avoid charging. Thermogravimetric analysis (TGA) was performed to ascertain the thermal stability and quantify the active content in the microcapsules. TGA analysis was carried out using Perkin Elmer's STA 6000 Instrument at a heating rate of 20 °C min under nitrogen atmosphere.

3.2. Extraction of active ingredient from microcapsules

0.2 g to 0.5 g of dry microcapsule sample containing active agent was weighed accurately and transferred to a 100 ml round bottom flask. 30 mL of 50% (v/v) of aqueous methanol was added to this flask and refluxed for 4 h. After refluxing, mixture was cooled to room temperature and filtered through Grade-3 sintered glass crucible; the residue was washed with 20–30 mL of 50% (v/v) aqueous methanol. Filtrate was transferred to 100 mL volumetric flask and further diluted with distilled water up to the mark. Further dilutions of this solution were made till concentration of final diluted solution fitted within the calibration range. Final dilutions were made in duplicate and the absorbance at 251 nm (λ_{max} of DEET) was measured on UV spectrophotometer (Agilent model 89090A) and the concentration of active ingredient was obtained by using the following formula,

$$Active\ Ingredient\ (\%) = \frac{Dilution\ Factor \times Absorbance}{Calibration\ Slope \times mg\ of sample} \times 100$$

3.3. Release measurements

Release study of pristine and mCNF containing MICs was carried out in dissolution apparatus (LABINDIA- DS8000). In this study, 56 mg of microcapsules were dispersed in 400 mL of distilled water and stirred at 150 RPM and 30 °C for 30 h. After specific time intervals, 10 mL aliquots were taken out and replenished with same amount of fresh distilled water to maintain concentration gradient. Absorbance of the aliquots were recorded using UV–vis spectrophotometer (Agilent model 89090A) at $\lambda max = 251$ nm to measure % release of DEET from MICs. The maximum amount of DEET in the reservoir was never above 28 mg which corresponds to a concentration of 70 ppm. This is an order of magnitude lower concentration than the solubility limit of DEET in water (1000 ppm). When five to ten fold higher volume of dissolution media is used than the saturation limit ("perfect sink" condition), it ensures that the dissolution rates do not reduce significantly over time due to solubility issues and cause inaccuracy in release data.

4. Results and discussion

4.1. Extraction and modification of CNFs

CNFs were prepared by mechanical grinding of bleached cotton rag pulp. TEM images (Fig. 1) confirm the formation of nanofibers with diameter in the range of 10–50 nm. TEM images of mCNF shows that the chemical modification did not affect the morphology of the fibers.

Due to aggregation of nanofibrils, the fiber diameter appeared to be slightly higher. The average diameter of mCNF still remained below 100 nm after the modification (Fig. 1b). In the FTIR spectrum (Fig. 2), the significant difference in the spectrum of mCNF and CNF is the band peak appearing at 1751 cm^{-1} corresponding to -C = O (ester) symmetric stretching. The -C = O band peak for stearic acid appears at 1698 cm^{-1}. Sharp increase in the asymmetric and symmetric $-CH_2$ stretching appearing at 2921 cm^{-1} and 2853 cm^{-1}, respectively,

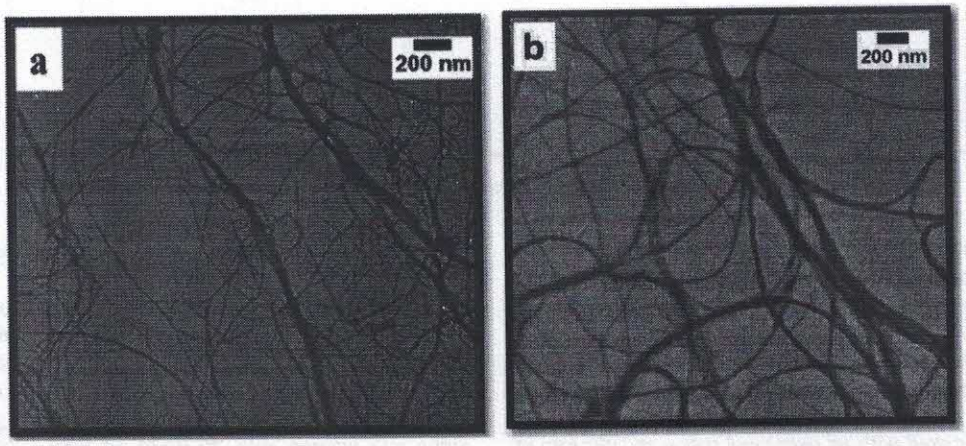

Fig. 1. TEM Image of (a) cellulose nanofibers and (b) modified cellulose nanofiber.

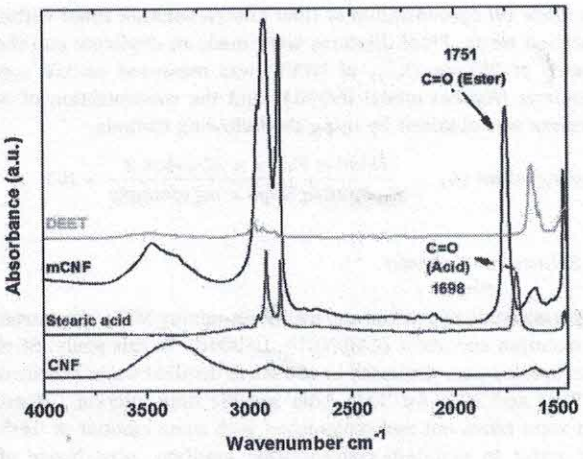

Fig. 2. FTIR spectrum of cellulose nanofibers, modified cellulose nanofibers and stearic acid.

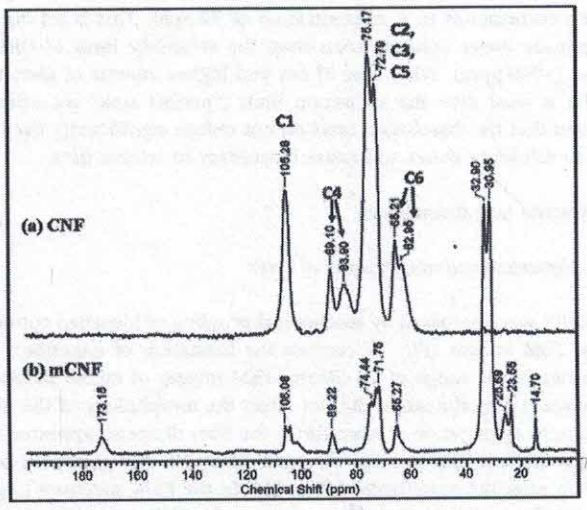

Fig. 3. ^{13}C Solid state NMR of cellulose nanofiber (CNF) and modified cellulose nanofibers (mCNF).

corresponds to the aliphatic chain of stearic acid linked to cellulose. Cellulose in this region has a broad band peak corresponding to −CH stretching [38] at 2902 cm^{-1}. In ^{13}C solid-state NMR (Fig. 3), the peak appearing at 173 ppm confirms the presence of -C = O ester bond, which is not present in neat CNFs. The peaks appearing close to 14, 23, 31 and 33 ppm correspond to the long aliphatic chain of stearic acid linked to cellulose along with cellulose backbone peaks appearing at 106.08, 89.22, 74.44-71.75 and 65.27 ppm corresponding to C1, C4, C2/C3/C5, and C6 carbon respectively [39]. The hydrophilic/hydrophobic character of nanocellulose was ascertained by measuring the contact angle using sessile water drop technique. The free OH groups in unmodified CNF imparts hydrophilic character.

Acetic anhydride, silanes, silica and amines have been used previously for chemically modifying nanocellulose. A considerable increase in contact angle (from 30-35°) upto 160° has been achieved using these modifiers indicating a clear hydrophobic character [40–44]. Huang et al. have used stearic acid for modifying nanocellulose and improve the dispersibility. However, there is no information on the effect of stearic acid on contact angle [45]. In our work, the unmodified CNF showed a lower contact angle of 53.5°as shown in Fig. 4a, whereas in case of mCNF, due to the covalently bound stearic acid, the contact angle increases significantly to 112.2° confirming hydrophobic surface characteristics (Fig. 4b).

4.2. Preparation of emulsion and MICs

Prior to actual encapsulation, emulsion studies were carried out with mCNF and Hypermer A60. Fig. 5 shows the optical images (**a-c**) and fluorescence microscopy images (**d-f**) of emulsion. When Hypermer A60 was used as a surfactant the emulsion size obtained was in the range of 1–5 μm (Fig. 5a&d), while CNFs as a pickering emulsifier led to droplets in

the range of 5–50 μm (Fig. 5b&e). However, when this emulsion was homogenized for 5 min at 11,000 rpm, the emulsion size obtained was in the range of 1–5 μm (Fig. 5c&f). For fluorescence microscopy, 0.5 mg/mL of Rhodamine B was used along with DEET. After confirming the successful action of mCNF as a surfactant in oil-in-oil emulsion, we attempted to encapsulate DEET, a mosquito repellant using interfacial polycondensation reaction. Fig. 6 shows the SEM images of MICs prepared using Hypermer A60 and mCNF. Good spherical and smooth microcapsules were obtained with varying proportion of mCNF (0.5, 1 and 2 wt%). The size of the MICs obtained was in the range of 1–12 μm with majority of the MICs in the range of 1–3 μm when the emulsion was homogenized. However, the size of MICs were higher (~ 80–100 μm) when emulsion was not homogenized.

4.3. Extraction analysis of active ingredients

The encapsulation efficiency of DEET was estimated using extraction studies. Experiments were conducted using 50% (v/v) aqueous methanol as described in the literature [28]. The DEET content was in the range of 46–49 wt%. The values obtained were in close agreement to the theoretical loading of DEET (50% by weight) (Table 1).

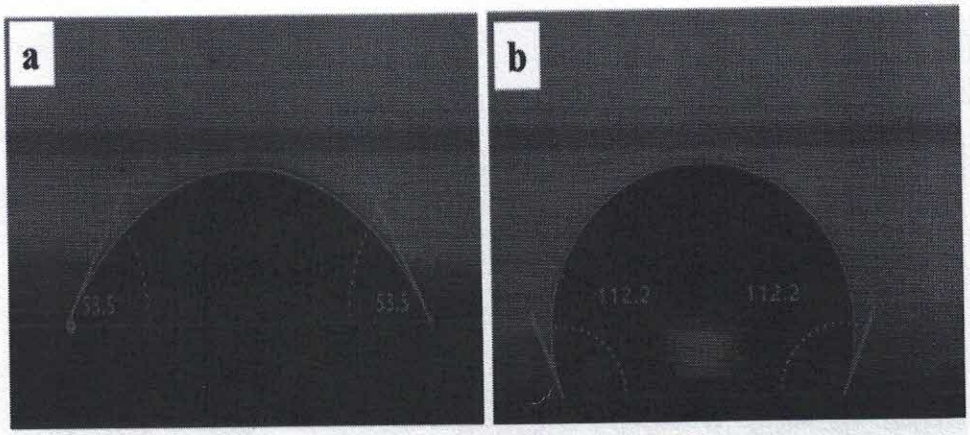

Fig. 4. Contact angle image of a) cellulose nanofiber and b) modified cellulose nanofiber.

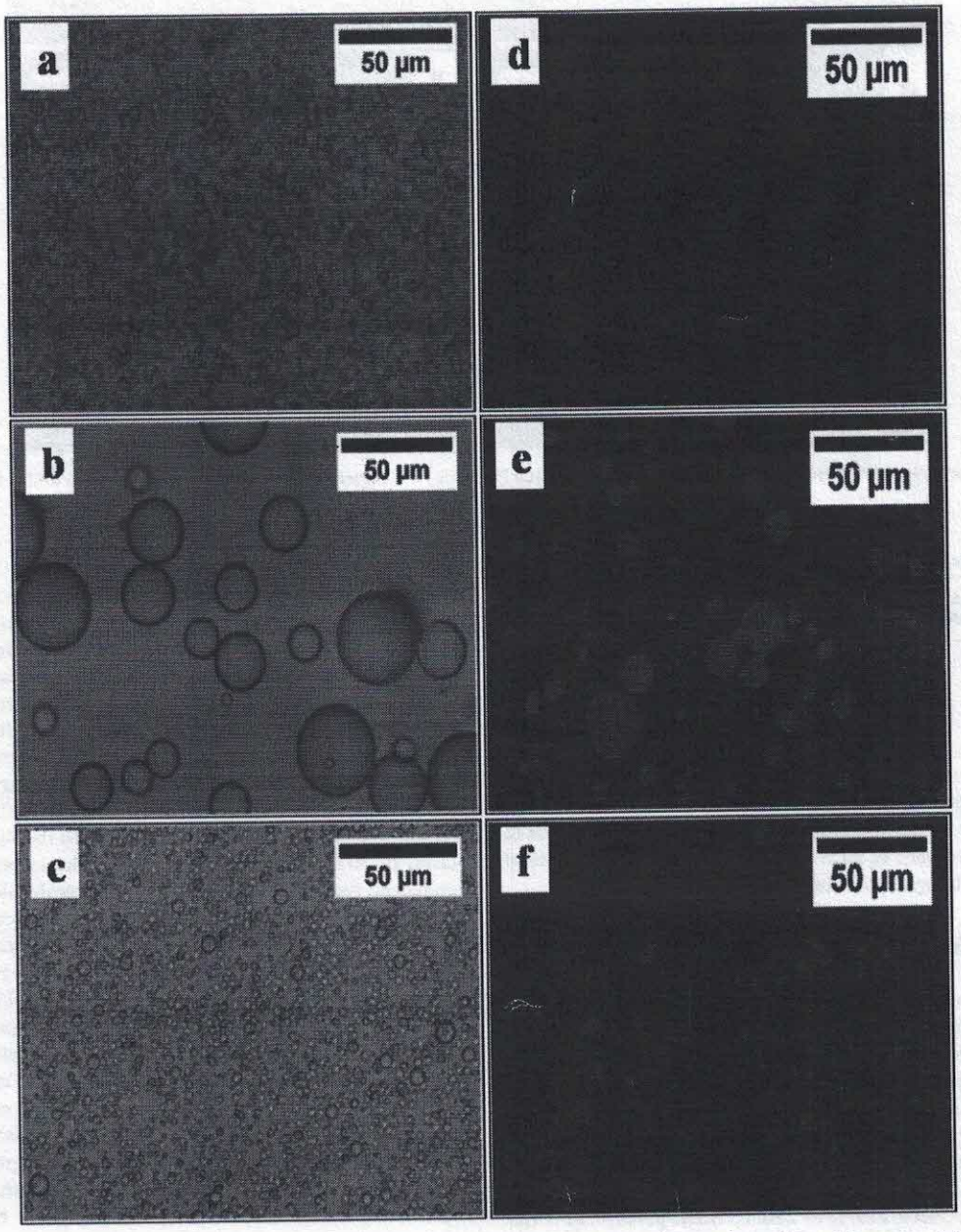

Fig. 5. Optical microscope images (a–c) and fluorescence optical microscope images (d–f) of the emulsion using surfactant hypermer A-60 (a,d), mCNF (b,e), and mCNF with homogenization (c,f).

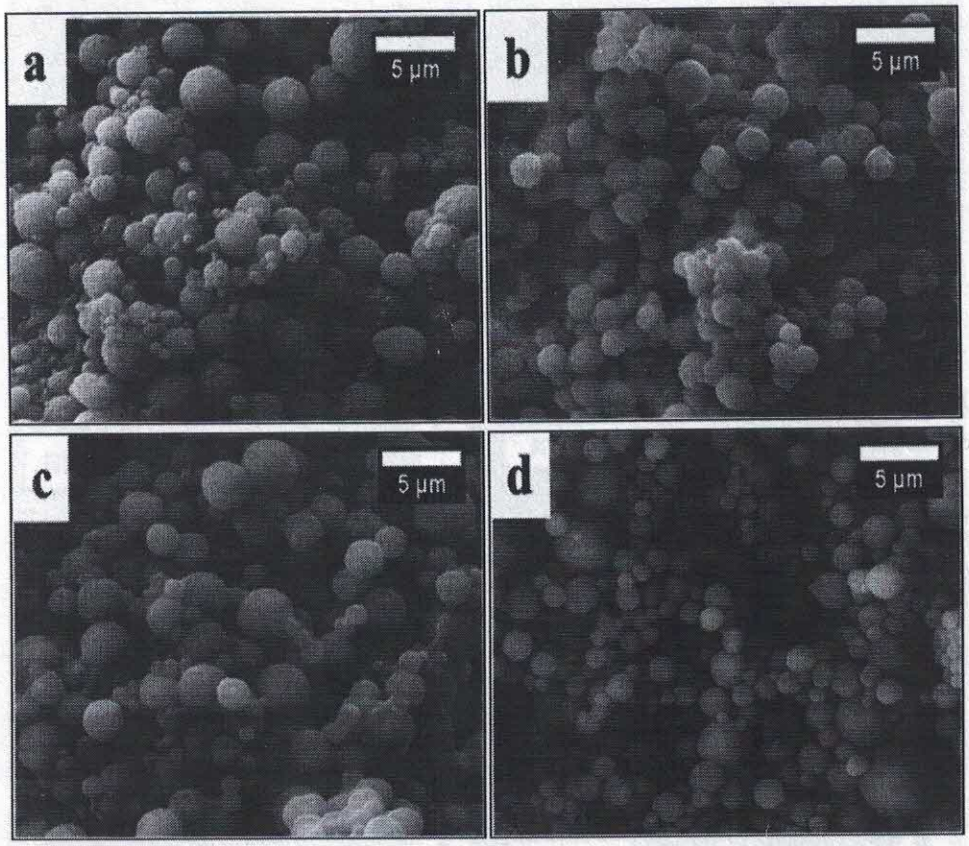

Fig. 6. Scanning electron micrographs of DEET encapsulated MICs (a) MICs with Hypermer A60 (b) 0.5% mCNF (c) 1% mCNF (d) 2% mCNF.

Table 1
Extraction of DEET from the polyurethane microcapsules.

Sample No.	Theoretical Loading (%)	Obtained Loading (%)	Encapsulation efficiency (%)
MICs-Hypermer	50	49	98
MICs-0.5%mCNF	50	46	92
MICs-1%mCNF	50	48	96
MICs-2%mCNF	50	49	98

The overall encapsulation efficiency achieved was about 92–98 %, which is significantly higher than that obtained with other methods of encapsulation. The presence of mCNF helped to prolong the release of DEET as shown in subsequent sections.

4.4. Thermogravimetric analysis

TGA was carried out to study the effect of mCNFs on the thermal stability of MICs and for confirming the encapsulation efficiency [46,47]. Fig. 7 represents the thermogram of MICs with and without mCNF. Two step degradation was observed for all the MICs.

The first degradation from 230 °C to 300 °C can be ascribed to the loss of DEET from the capsules [41], while the second degradation step is due to polymer decomposition. From the differential thermogravimetric analysis (Fig. 7b), we can observe that the decomposition of DEET alone occurs between 115 °C to 250 °C, while polyurethane microspheres without any DEET decomposes between 230 °C to 350 °C (denoted as MIS). In the case of MICs, we could observe a shift in the decomposition of DEET to higher temperatures and the decomposition also overlapped with the decomposition peak of polymer.

Hence it was difficult to accurately estimate the DEET content in the MICs using TGA. We could at least conclude that encapsulation delays the thermal decomposition of DEET.

4.5. Release study of DEET from MICs

Percentage release of DEET from the pristine and mCNF embedded MICs was determined using procedure reported in the literature [40,48,49]. Experiments were repeated four times and the average values have been used in the release curves depicted in Fig. 8. Pristine MICs prepared using Hypermer A60 showed faster release of DEET with about 70% cumulative release occurring in 30 h. On the other hand mCNF reinforced MICs showed significantly slower release of DEET. The incorporation of mCNF also led to sharp decrease in the burst release observed during the first six hours (Fig. 8b). Among all mCNF reinforced MICs, 2% mCNF/MICs exhibited the slowest release of DEET (23% in 30 h).This can be ascribed to the increase in tortuosity and enhanced barrier to permeation of small molecules through the mCNF reinforced microcapsule wall. Increase in mCNF concentration from 1% to 2% led to slight increase in barrier properties. Further increase in mCNF did not show much difference in the release behavior of DEET. Similar observation was reported by Jagtap et al [46]. The cumulative release reduced by almost 20% (as compared to pristine MICs) by using polyurea MICs with 2% clay. On increasing the clay content to 4%, the release rate also increased. Yoo et al. [50] have also demonstrated the use of polylactic acid modified nano crystals for controlling the release of an active ingredient from poly (urea-urethane) MICs. However, the release rate of the active ingredient reduced progressively on increasing the concentration of modified nanocrystals in the polymer from 0 to 7.5%. The maximum reduction in cumulative release achieved was close to 20%.

4.6. Mathematical interpretation

We also attempted to interpret the release data using established mathematical models and further understand the mechanism governing the release of active ingredient from microcapsules [51]. When the

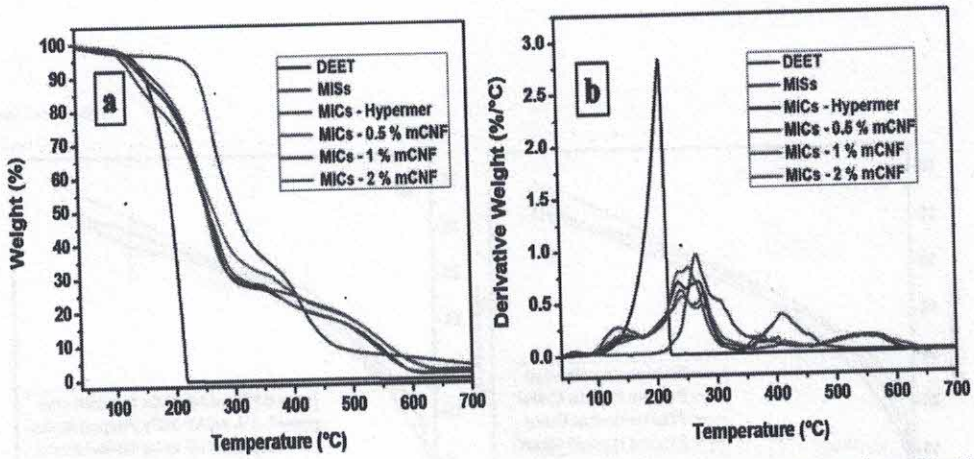

Fig. 7. (a) TGA and (b) differential thermogravimetry curves of DEET, MISs, hypermer MICs and 0.5, 1, and 2 wt % mCNF MJCs.

encapsulated active ingredient is hydrophilic the controlling mechanism is often diffusion, while for hydrophobic active ingredients, swelling or matrix erosion can also govern the release of active [52]. Since DEET has substantial solubility in water (1000 ppm) and the polyurethane shell is relatively hydrophobic in nature, we hypothesized that the release is likely to be diffusion controlled. Thus, the Higuchi equation [53] was first attempted for fitting the experimental release profile.

$$Q = k_H \sqrt{t} \tag{1}$$

Where, Q represents the amount of active released and k_H is the Higuchi constant (or release rate constant). The major assumption in this model is that the release rate remains constant throughout. This is valid only when the capsules do not swell significantly and the path for diffusion (diffusional resistance) remains the same throughout the release period. Table 2 (rows 1 to 4) shows the values for the rate constant k_H and the correlation coefficient (R^2) for release profiles of all the four samples. Increase in the concentration of nanofiber in the polymer shell led to a steady decline in the values of k_H indicating higher diffusional resistance of polymeric shell embedded with mCNF. However, the R^2 value decreased steadily with increase in mCNF. Hence, we explored other mathematical equations. The power law described by Korsmeyer, Ritger and Peppas is a semi-empirical equation which can explain the release of active ingredient from polymeric systems more comprehensively [54,55].

$$\frac{M_i}{M_\infty} = K.\, t^n \tag{2}$$

Where M_i/M_∞ is the fraction of active released at time t, K is the release rate constant and n is the exponent of time t which represents the mechanism of release. This model predicted the release profiles very well. Table 2 (rows 5 to 8) shows the K, n and R^2 values for all four batches. The K value decreased almost by a factor of three on incorporating 0.5 wt% of mCNF, indicating the strong influence of cellulose nanofibers on the barrier properties of the polymer shell. Further increase in concentration of mCNF did not change the K value significantly. This trend can also be observed in the release profiles, where the microcapsules incorporated with mCNF have release profiles which are drastically slower than the pristine MICs but almost closer to each

Table 2
Parameters for different mathematical models used to fit experimental release profiles.

Model	Sr. No.	Concentration of mCNF (wt %)	k_H		R^2
Higuchi	1	0 (Pristine)	1.62		0.97
	2	0.5	0.83		0.95
	3	1	0.70		0.92
	4	2	0.53		0.90
Korsmeyer, Ritger and Peppas		**Concentration of mCNF (wt %)**	**K**	**n**	**R^2**
	5	0 (Pristine)	0.053	0.33	0.9921
	6	0.5	0.017	0.39	0.9823
	7	1	0.019	0.35	0.9908
	8	2	0.016	0.36	0.9778
Weibull Model		**Concentration of mCNF (wt %)**	**a**	**b**	**R^2**
	9	0 (Pristine)	0.020	0.52	0.9928
	10	0.5	0.014	0.44	0.9846
	11	1	0.017	0.38	0.9914
	12	2	0.014	0.39	0.9802

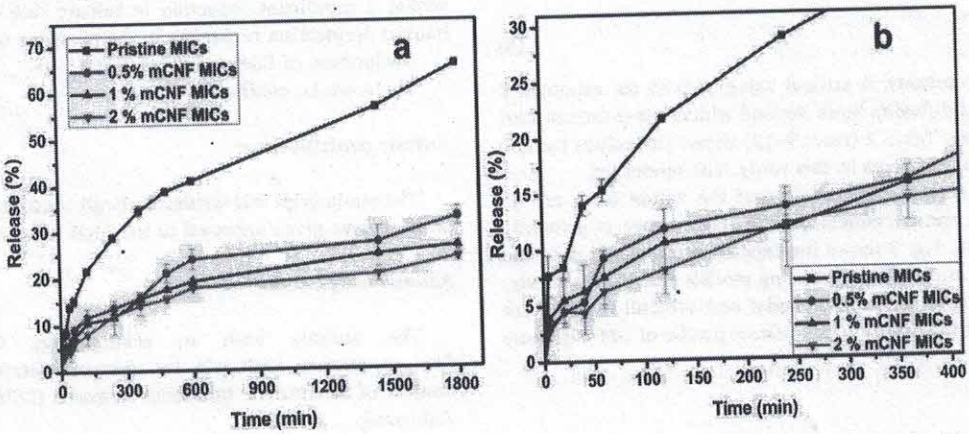

Fig. 8. Release behavior of DEET from microcapsules in distilled water at room temperature (a) overall release (b) initial release.

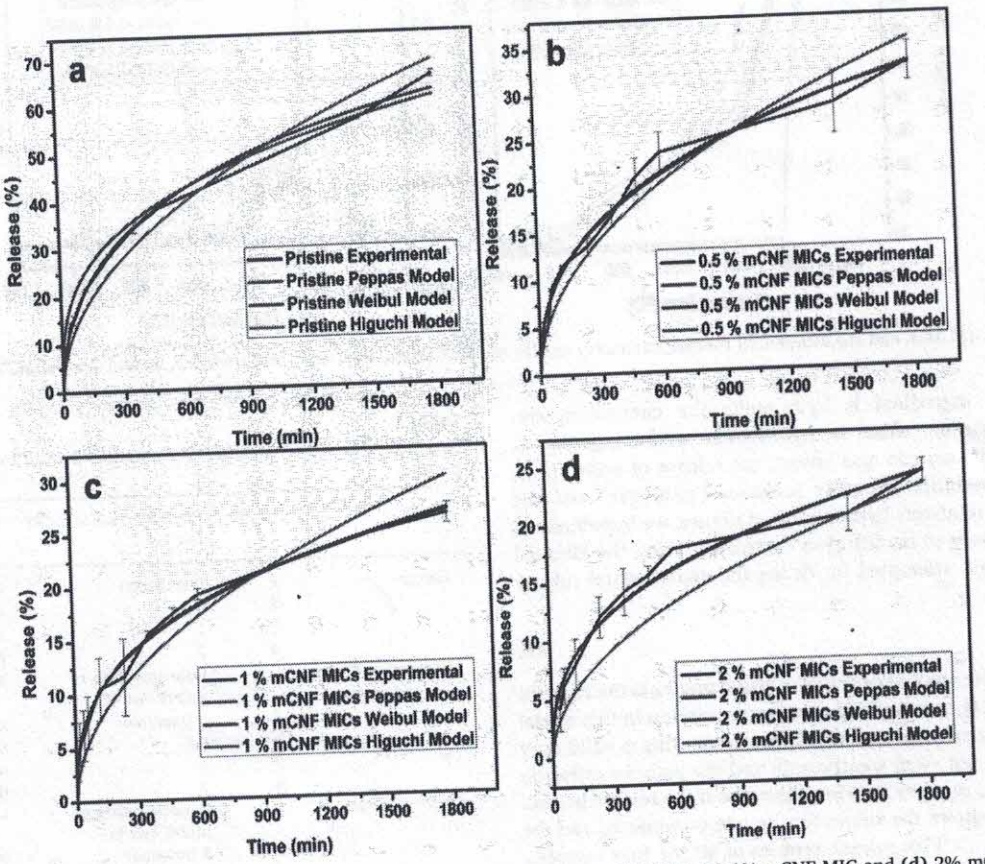

Fig. 9. Experimental and predicted release profiles for **(a)** pristine **(b)** 0.5% mCNF MIC, **(c)** 1% mCNF MIC and **(d)** 2% mCNF MIC.

other. The exponent '*n*' in the Korsmeyer–Peppas model is lower than 0.43 which generally indicates a deviation from the Fickian range of diffusion. However Ritger and Peppas obtained values as low as 0.3 for Fickian materials which were polydisperse [45]. They concluded that a specific range of n cannot be defined for samples having particle size distribution.

We also explored the Weibull model which was first introduced in 1951 [56] and applied to drug release systems in 1972 [57]. Papadopoulou et al. have used computer simulations for determining the mechanisms of controlled release curves using the following form of the Weibull function [58].

$$\frac{M_i}{M_\infty} = 1 - exp(-a.\ t^b) \quad (3)$$

where a and b are constants. A critical value of 0.75 for exponent b represents the Fickian diffusion limit, beyond which, other factors start influencing the release. Table 2 (rows 9–12) shows the values for a, b and R^2 fitted to all four systems in this study. The model fits

all the four MIC release curves well and the values for b are all below 0.75. Thus, it can be concluded that the release is primarily controlled by diffusion. Fig. 9 shows the experimental release data and the predicted release curves obtained using models discussed hitherto. Among the models explored, Peppas model and Weibull model were able to closely predict the experimental release profile of DEET in these MICs.

5. Conclusions

This study illustrates that hydrophobically modified cellulose nanofibers could be used as an ecofriendly alternative to perform dual functions, viz stabilize emulsions as well as prolong the release of active ingredients from microcapsules. Although few reports are available on microencapsulation of DEET, they are not based on pickering emulsions or nanocomposite microcapsules by interfacial polycondensation, a process that can lead to high encapsulation efficiency. Here, we report on the successful encapsulation of DEET by interfacial polycondensation using mCNF as pickering emulsifier. This approach enabled to achieve a high encapsulation efficiency of around 92–98%. Microcapsules obtained by this approach were spherical and smooth with size ranging from 5 to 40 μm. Thermogravimetric analysis of MICs indicate a delayed decomposition of DEET upon encapsulation. Presence of mCNF led to a significant reduction in the release rate c DEET. Interpretation of release profile by standard mathematical models such as Higuchi, Korsemayer-Ritger–Peppas and Weibull revealed a significant reduction in release rate constants implying enhanced permeation resistance in the presence of mCNF.

Declaration of Competing Interest

There are no conflicts to declare.

Author contributions

The manuscript was written through contributions of all authors. All authors have given approval to the final version of the manuscript.

Acknowledgements

The authors wish to acknowledge Centre for Material Characterization, CSIR-NCL for characterization facilities. SK thanks Council of Scientific & Industrial Research (CSIR) for Junior Research Fellowship.

References

[1] A. Abbaspourrad, S.S. Datta, D.A. Weitz, Controlling release from pH-responsive microcapsules, Langmuir 29 (2013) 12697–12702.
[2] I.M. Martins, S.N. Rodrigues, M.F. Barreiro, A.E. Rodrigues, Release of thyme oil from polylactide microcapsules, Ind. Eng. Chem. Res. 50 (2011) 13752–13761.

[3] G. Choudhary, J. Kumar, S. Walia, R. Parsad, B.S. Parmar, Development of controlled release formulations of carbofuran and evaluation of their efficacy against meloidogyneincognita, J. Agric. Food Chem. 54 (2006) 4727–4733.

[4] N.V.N. Jyothi, P. Muthu Prasanna, S.N. Sakarkar, K. Surya Prabha, P. Seetha Ramaiah, G.Y. Srawan, Microencapsulation techniques, factors influencing encapsulation efficiency, J. Microencapsul. 27 (2010) 187–197.

[5] C.A. Finch, Industrial microencapsulation: polymers for microcapsule walls, in: D.R. Karsa, R.A. Stephenson (Eds.), Encapsulation and Controlled Release, Woodhead Publishing Series in Food Science, Technology and Nutrition, Woodhead Publishing, 2005, pp. 1–12.

[6] P.G. Shukla, S.B. Jagtap, S.C. Biradar, V.P. Charpe, A.S. Jadhav, Preparation and characterization of microcapsules containing industrially important reactive water-soluble polyamine, Colloid Polym. Sci. 294 (2016) 2039–2050.

[7] P.G. Shukla, B. Kalidhass, A. Shah, D.V. Palaskar, Preparation and characterization of microcapsules of water-soluble pesticide monocrotophos using polyurethane as carrier material, J. Microencapsul. 19 (2002) 293–304.

[8] A. Schoth, K. Landfester, R. Muñoz-Espí, Surfactant-free polyurethane nanocapsules via inverse pickering miniemulsion, Langmuir 31 (2015) 3784–3788.

[9] M. Gestranius, P. Stenius, E. Kontturi, J. Sjöblom, T. Tammelin, Phase behaviour and droplet size of oil-in-water Pickering emulsions stabilized with plant-derived nanocellulosic materials, Colloids Surf. A Physicochem. Eng. Asp. 519 (2017) 60–70.

[10] H. Liu, S. Geng, P. Hu, Q. Qin, C. Wei, J. Lv, Study of pickering emulsion stabilized by sulfonated cellulose nanowhiskers extracted from sisal fiber, Colloid Polym. Sci. 293 (2015) 963–974.

[11] M. Andresen, P. Stenius, Water-in-oil emulsions stabilized by hydrophobized microfibrillated cellulose, J. Disper. Sci. Technol. 28 (2007) 837–844.

[12] B.P. Binks, S.O. Lumsdon, Catastrophic phase inversion of water-in-oil emulsions stabilized by hydrophobic silica, Langmuir 16 (2000) 2539–2547.

[13] B.P. Binks, C.P. Whitby, Silica particle-stabilized emulsions of silicone oil and water: aspects of emulsification, Langmuir 20 (2004) 1130–1137.

[14] A. Gelot, W. Friesen, H.A. Hamza, Emulsification of oil and water in the presence of finely divided solids and surface active agents, Colloids Surf. 12 (1984) 271–303.

[15] J.H. Schulman, J. Leja, Control of contact angles at the oil-water-solid interfaces emulsions stabilized by solid particles ($BaSO_4$), Trans. Faraday Soc. 50 (1954) 598–605.

[16] D.E. Tambe, M.M. Sharma, Factors controlling the stability of colloid-stabilized emulsions. I. An experimental investigation, J. Colloid Interface Sci. 157 (1993) 244–253.

[17] L. Bai, W. Xiang, S. Huan, O.J. Rojas, Formulation and stabilization of concentrated edible oil-in-water emulsions based on electrostatic complexes of a food-grade cationic surfactant (ethyl lauroyl arginate) and cellulose nanocrystals, Biomacromolecules 19 (2018) 1674–1685.

[18] A.G. Cunha, J. Mougel, B. Cathala, L.A. Berglund, I. Capron, Preparation of double pickering emulsions stabilized by chemically tailored nanocelluloses, Langmuir 30 (2014) 9327–9335.

[19] X. Gong, Y. Wang, L. Chen, Enhanced emulsifying properties of wood-based cellulose nanocrystals as pickering emulsion stabilizer, Carbohydr. Polym. 169 (2017) 295–303.

[20] C. Salas, T. Nypelö, C. Rodriguez-Abreu, C. Carrillo, O.J. Rojas, Nanocellulose properties and applications in colloids and interfaces, Curr. Opin. Colloid Interface Sci. 19 (2014) 383–396.

[21] X. Lia, J. Lia, J. Gonga, Y. Kuanga, L. Moa, T. Songa, Cellulose nanocrystals (CNCs) with different crystalline allomorph for oil in water pickering emulsions, Carbohydr. Polym. 183 (2018) 303–310.

[22] D. Saidane, E. Perrin, F. Cherha, F. Guellec, I. Capron, Some modification of cellulose nanocrystals for functional Pickering emulsions, Philos. Trans. Math. Phys. Eng. Sci. 374 (2016) 20150139.

[23] B.P. Binks, Particles as surfactants-similarities and differences, Curr. Opin. Colloid Interface Sci. 7 (2002) 21–41.

[24] M. Zembyla, B.S. Murray, A. Sarkar, Water-in-oil pickering emulsions stabilized by water-insoluble polyphenol crystals, Langmuir 34 (2018) 10001–10011.

[25] D. Yu, X. Zheng, Y. Yang, X. Li, G.R. Williams, M. Zhao, Immediate release of helicid from nanoparticles produced by modified coaxial electrospraying, Appl. Surf. Sci. 473 (2019) 148–155.

[26] K. Wang, H. Wen, D. Yu, Y. Yang, D. Zhang, Electrosprayed hydrophilic nanocomposites coated with shellac for colon-specific delayed drug delivery, Mater. Des. 143 (2018) 248–255.

[27] T. Hai, X. Wan, D. Yu, K. Wang, Y. Yang, Z. Liu, Electrospun lipid-coated medicated nanocomposites for an improved drug sustained-release profile, Mater. Des. 162 (2019) 70–79.

[28] X. Li, Z. Zheng, D. Yu, X. Liu, Y. Qu, H. Li, Electrosprayed spherical ethylcellulose nanoparticles for an improved sustained-release profile of anticancer drug, Cellulose 24 (2017) 5551–5564.

[29] G.M. Gomes, J.P. Bigon, F.E. Montoro, L.M.F. Lona, Encapsulation of N,N -diethylmeta -toluamide (DEET) via miniemulsion polymerization for temperature controlled release, J. Appl. Polym. Sci. 136 (2019) 47139–47149.

[30] S.S. Kulkarni, M.S. Mohan, S.B. Jagtap, R.G. Dandage, A.S. Jadhav, P.G. Shukla, Polyurea and polyurethane microcapsules containing mosquito repellent DEET: preparation and characterization, Appl. Sci. Adv. Mater. Int. 2 (2015) 7–10.

[31] Z. Zhang, K.C. Tam, X. Wang, G. Sèbe, Inverse pickering emulsions stabilized by cinnamate modified cellulose nanocrystals as templates to prepare silica colloidosomes, ACS Sustain. Chem. Eng. 6 (2018) 2583–2590.

[32] W. Chen, H. Yu, Y. Liu, P. Chen, M. Zhang, Y. Hai, Individualization of cellulose nanofibres from wood using high-intensity ultrasonication combined with chemical pretreatments, Carbohydr. Polym. 83 (2011) 1804–1811.

[33] W. Chen, K. Abe, K. Uetani, H. Yu, Y. Liu, H. Yano, Individual cotton cellulose nanofibres: pretreatment and fibrillation technique, Cellulose 21 (2014) 1517–1528.

[34] M.D. Patil, V.D. Patil, A.A. Sapre, T.S. Ambone, A.T. Torris, P.G. Shukla, K. Shanmuganathan, Tuning controlled release behavior of starch granules using nanofibrillated cellulose derived from waste sugarcane bagasse, ACS Sustain. Chem. Eng. 6 (2018) 9208–9217.

[35] S. Sharma, S.S. Nair, Z. Zhang, A.J. Ragauskas, Y. Deng, Characterization of microfibrillation process of cellulose and mercerized cellulose pulp, RSC Adv. 5 (2015) 63111–63122.

[36] P. Jandura, B. Riedl, B.V. Kokta, Thermal degradation behavior of cellulose fibers partially esterified with some long chain organic acids, Polym. Degrad. Stabil. 70 (2000) 387–394.

[37] **P.G. Shukla, A.S. Jadhav, Microcapsules containing water soluble amine and process for the preparation thereof. US 0325448 A1, 2017.**

[38] E. Krasnou, T. Tarasova, T. Märtson, A. Krumme, Thermoplastic cellulose stearate and cellulose laurate: melt rheology, processing and application potential, Int. Polym. Process. J. Polym. Process. Soc. 30 (2015) 210–216.

[39] A. Geissler, D. Scheid, W. Li, M. Gallei, K. Zhang, Facile formation of stimuli-responsive, fluorescentand magnetic nanoparticles based on cellulose stearoyl ester via nanoprecipitation, Cellulose 21 (2014) 4181–4194.

[40] M. Jonoobi, J. Harun, A.P. Mathew, M.B. Hussien, K. Oksman, Preparation of cellulose nonofibres with hydrophobic surface characteristics, Cellulose 17 (2010) 299–307.

[41] M.M. Bashar, H. Zhu, S. Yamamoto, M. Mitsuishi, Superhydrophobic surfaces with fluorinated cellulose nanofibre assemblies for oil-water separation, RSC Adv. 7 (2017) 37168–37174.

[42] N.T. Cervin, C. Aulin, P.T. Larsson, L. Wagberg, Ultra porous nanocellulose aerogels as separation medium for mixtures of oil/water liquids, Cellulose 19 (2012) 401–410.

[43] D. Le, S. Kongparakul, C. Samart, P. Phanthong, S. Karnjanakom, A. Abudula, G. Guan, One-pot fabrication of hydrophobic nanocellulose-silica film for water resistant packaging application, J. Jpn. Inst. Energy 96 (2017) 361–365.

[44] R.K. Johnson, A. Zink-Sharp, W.G. Glasser, Preparation and characterization of hydrophobic derivatives of TEMPO-oxidized nanocelluloses, Cellulose 18 (2011) 1599–1609.

[45] L. Huang, X. Zhang, M. Xu, J. Chen, Y. Shi, C. Huang, S. Wang, S. An, C. Li, Preparation and mechanical properties of modified nanocellulose/PLA composites from cassava residue, AIP Adv. 8 (2018) 025116.

[46] S.B. Jagtap, M. Subramanian, P.G. Shukla, Improved performance of microcapsules with polymer nanocomposite wall: preparation and characterization, Polymer 83 (2016) 27–33.

[47] W. Jing, L. Yafei, Y. Huilin, Effects of plasticizers and stabilizers on thermal stability of polyvinyl fluoride, Polymer-Plastics Technol. Eng. 46 (2007) 461–468.

[48] P.G. Shukla, N. Rajgopalan, C. Bhaskar, S. Sivaram, Crosslinked starch-urea formaldehyde (St-UF) as a hydrophilic matrix for encapsulation: studies in swelling and release of carbofuran, J. Control. Release 15 (1991) 153–165.

[49] P.G. Shukla, N. Rajagopalan, S. Sivaram, Starch urea-formaldehyde matrix encapsulation. IV. Influence of solubility and physical state of encapsulant on rate and mechanism of release, J. Appl. Polym. Sci. 48 (1993) 1209–1222.

[50] Y. Yoo, C. Martinez, J.P. Youngblood, Synthesis and Characterization of microencapsulated phase change materials with Poly(urea−urethane) shells containing cellulose nanocrystals, ACS Appl. Mater. Interfaces 9 (2017) 31763–31776.

[51] M. Bruschi, Mathematical models of drug release, in: M. Bruschi (Ed.), Strategies to Modify the Drug Release from Pharmaceutical Systems, Elsevier/Woodhead Publishing, Amsterdam, 2015, pp. 63–86.

[52] E.J. Agnes, G. Gonzales Ortega, Mathematical models and physicochemical of diffusion, Pharmacy Book 19 (2003) 9–19.

[53] T. Higuchi, Rate of release of medicaments from ointments bases containing drugs in suspension, J. Pharm. Sci. 50 (1961) 874–875.

[54] R.W. Korsmeyer, R. Gurny, E.M. Doelker, P. Buri, N.A. Peppas, Mechanism of solute release from porous hydrophilic polymers, Int. J. Pharm. 15 (1983) 25–35.

[55] P.L. Ritger, N.A. Peppas, A simple equation for describing of solute release. I. Fickian and non-Fickian release from non-swellable devices in the form of slabs, spheres, cylinders or discs, J. Control. Release 5 (1987) 23–36.

[56] W. Weilbull, A statistical distribution function of wide applicability, J. Appl. Mech. 18 (1951) 293–297.

[57] F. Langenbucher, Linearization of dissolution rate curves by the Weibull distribution, J. Pharm. Pharmacol. 24 (1972) 979–981.

[58] V. Papadopoulou, K. Kosmidis, M. Vlachou, P. Macheras, On the use of the Weibull function for the discernment of drug release mechanisms, Int. J. Pharm. 309 (2006) 44–50.